How to cite: *Angew. Chem. Int. Ed.* **2024**, *63*, e202410928
doi.org/10.1002/anie.202410928

Photocatalysis

Organocatalyzed Carbonylation of Alkyl Halides Driven by Visible Light

Xin Liu[+], Brandon S. Portela[+], Analiese Wiedenbeck, Cameron H. Chrisman, Robert S. Paton, and Garret M. Miyake**

Abstract: Herein, we describe a new strategy for the carbonylation of alkyl halides with different nucleophiles to generate valuable carbonyl derivatives under visible light irradiation. This method is mild, robust, highly selective, and proceeds under metal-free conditions to prepare a range of structurally diverse esters and amides in good to excellent yields. In addition, we highlight the application of this activation strategy for ^{13}C isotopic incorporation. We propose that the reaction proceeds by a photoinduced reduction to afford carbon-centered radicals from alkyl halides, which undergo subsequent single electron-oxidation to form a carbocationic intermediate. Carbon monoxide is trapped by the carbocation to generate an acylium cation, which can be attacked by a series of nucleophiles to give a range of carbonyl products.

Introduction

Using carbon monoxide (CO) as a C1 building block in carbonylation for the synthesis of various carbonyl compounds, such as aldehydes, acids, esters, and amides is a powerful reaction.[1] In general, these processes make use of transition-metal-catalysts under high temperatures and pressures, requiring specific equipment and safety measures. To overcome these challenges, various methodologies have been developed in the field of carbonylation chemistry. Driven by the continuous demand for sustainable organic synthesis, photocatalysis has emerged as a powerful manifold for carbonylation reactions.[2]

The early development of photocatalytic carbonylation of organic halides required transition-metal catalysts, high-energy irradiation, and high pressures of CO gas.[3] Although metal-free catalytic systems have been developed for carbonylation,[4] they are still hampered by the need for specialized apparatus and high-energy light sources. In recent years, the situation has changed dramatically thanks to the maturation of photoredox catalysis. Several catalytic systems for the carbonylation of organic halides have been successfully developed harnessing photoredox catalysis under visible light (Figure 1a), using cobalt,[5] nickel,[6] iridium,[7] manganese,[8] and palladium-based systems.[9] However, no general strategy has been developed for the direct carbonylation of organic halides to various carbonyl products.

In 2020, Arndtsen and co-workers developed a catalytic Pd system for the carbonylation of organic iodides and bromides, forming carbonyl derivatives under low pressure CO (4.0 bar) and visible-light conditions (Figure 1b).[10] Unlike classical carbonylation, both oxidative addition and reductive elimination steps in this strategy are driven by visible light through radical processes. Notably, after CO insertion, the highly reactive intermedi-

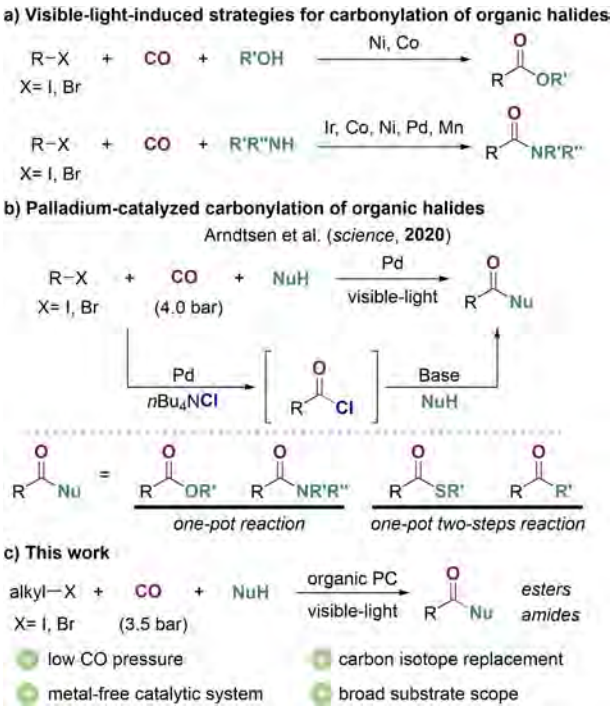

Figure 1. Carbonylation of organic halides via visible light. **NuH**: nucleophiles; **PC**: photoredox catalyst.

[*] Dr. X. Liu,[+] B. S. Portela,[+] A. Wiedenbeck, Dr. C. H. Chrisman, Prof. Dr. R. S. Paton, Prof. Dr. G. M. Miyake
Department of Chemistry, Colorado State University
Center Ave, Fort Collins, CO 80523, United States
E-mail: robert.paton@colostate.edu
garret.miyake@colostate.edu

[+] These authors contributed equally to this work.

ate acid chloride can be formed via chlorine abstraction. The acid chloride formed can react further with various nucleophiles either in situ or subsequently to produce amides, esters, thioesters, and ketones. Furthermore, in 2023, Arndtsen and co-workers also developed a Ni-catalytic system for the carbonylation of alkyl halides proceeding via acid chloride intermediates.[11] Although the utility of these two strategies is impressive, a transition metal catalyst is still required.

Considering the ever-increasing demands for sustainable chemical synthesis, particularly for processes of industrial relevance, a key challenge for carbonylation is to overcome the need for a transition metal catalyst while reducing energy consumption. Our interests in organic photoredox catalysis[12] motivated us to develop the carbonylation of organohalides under metal-free conditions. Along these lines, we took note of recent reports that visible-light organic photoredox catalysis can transform organic halides to various products via a radical generation strategy.[13] On this basis, we recognized an opportunity to design a unifying method for the direct carbonylation of organic halides to various products using organic photoredox catalysis. Herein, we report the organocatalyzed carbonylation of alkyl halides to esters and amides at low CO pressures driven by visible light (Figure 1c). This technology also presents a general strategy for complete ^{13}C isotopic incorporation.

Table 1: Optimization of reaction conditions.[a]

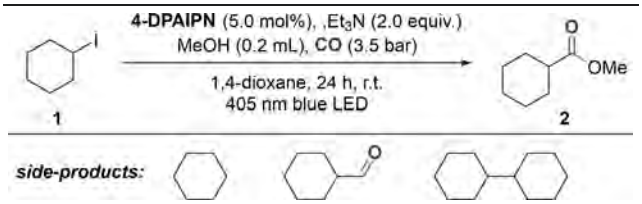

entry	Variation to standard conditions	2/%[b]	side-prod./%[b]
1	none	86	11
2	**NpMI** instead of **4-DPAIPN**	3	6
3	**eosin-Y** instead of **4-DPAIPN**	11	34
4	**PZ** instead of **4-DPAIPN**	9	18
5	**3CzClIPN** instead of **4-DPAIPN**	5	47
6	**3DPAFIPN** instead of **4-DPAIPN**	20	35
7	**4CzIPN** instead of **4-DPAIPN**	52	27
8	DIPEA instead of Et_3N	76	18
9	K_2CO_3 instead of Et_3N	3	0
10	no CO	0	33
11	no light, or no Et_3N	0	0
12	no **4-DPAIPN**	9	<3
13	$Mo(CO)_6$ instead of CO gas	71	28
14	$W(CO)_6$ instead of CO gas	10	47
15	CO (1.0 bar) used	39	31

[a] Reaction conditions: **1** (0.25 mmol), **4-DPAIPN** (5.0 mol%), Et_3N (0.5 mmol), CO gas (3.5 bar), MeOH (0.2 mL), 1,4-dioxane (1.0 mL), room temperature (21 °C), 405 nm LED. CO gas was introduced through a combination of SilaCOgen and CO balloon (see Supporting Information for more details). [b] The yield was determined by GC using mesitylene as the internal standard.

Results and Discussion

Reaction Development. We initiated our study using iodocyclohexane **1**, CO gas, and methanol (Table 1). The investigation identified the optimal standard conditions to use 2,4,5,6-tetrakis (diphenylamino)isophthalonitrile (**4-DPAIPN**) as the catalyst (3.0 mol%), Et_3N (2.0 equiv.), CO (3.5 bar), and MeOH (0.2 mL) in 1,4-dioxane (1.0 mL). Under these conditions, the corresponding ester product **2** was obtained in 86% yield (entry 1), with the main side products being cyclohexane, cyclohexyl carboxaldehyde, and bi-cyclohexyl. In this system, **4-DPAIPN** was particularly effective, and other well-known organic photoredox catalysts resulted in lower conversion and selectivity (entries 2–7). The use of *N*,*N*-diisopropylethylamine (DIPEA) instead of Et_3N also provided **2** in good yield, albeit with slightly diminished selectivity and conversion (entry 8). When K_2CO_3 was used as a base, only trace amounts of **2** were detected (entry 9). Control experiments revealed the essential roles of CO gas, irradiation, and electron donor, with no corresponding product being detected in their absence (entries 10 and 11). In the absence of photocatalyst, 9% of **2** was obtained, which could arise from an atom-transfer carbonylation (ATC) mechanism (entry 12). Notably, when using $Mo(CO)_6$ or $W(CO)_6$ instead of CO gas as the carbonyl source a good yield of **2** was obtained, but more side products were detected (entries 13 and 14). We noted that using 1.0 bar CO gas also gave a useful yield of **2** (entry 15). Other solvents, bases, and light were also studied but did not lead to an improvement in yields (see Supporting Information for more details, Table S2 to S4).

Reaction Scope. With the optimal reaction conditions in hand, we examined the substrate scope of this system (Figure 2). Moderate to good yields of the corresponding esters **2**–**11** were obtained, with yields up to 86% for a range of alkyl iodides as substrates while using methanol as the nucleophile. Several commonly encountered organic functional groups, such as amide (**5**), trifluoromethyl (**6**), aryl halides (**7** and **8**), thiophene (**9**), trifluoromethyl (**10**) and carbamate (**11**), proved compatible. Non-cyclic alkyl iodides were amenable to these conditions with the corresponding esters **12**–**15** obtained in good yield (54–74%, respectively). Furthermore, tertiary alkyl iodides could be smoothly converted into esters **16**–**18** in yield up to 70%.

Additionally, primary alkyl iodides gave low yields of the corresponding methyl esters under our standard conditions, with mostly homocoupled side products being detected. Therefore, we investigated the alkoxycarbonylation of primary iodide under different conditions (see Supporting Information for more details, Table S6). To our delight, primary iodides gave useful yields of corresponding products **19**–**21** up to 35% when Bn_3N was used instead of Et_3N and with THF as solvent. Turning to the alkyl bromide scope, we found that the use of DIPEA as the electron donor and MeCN as a co-solvent was crucial to ensure good reactivity (see Supporting Information for more details, Table S6). Using these conditions, we were

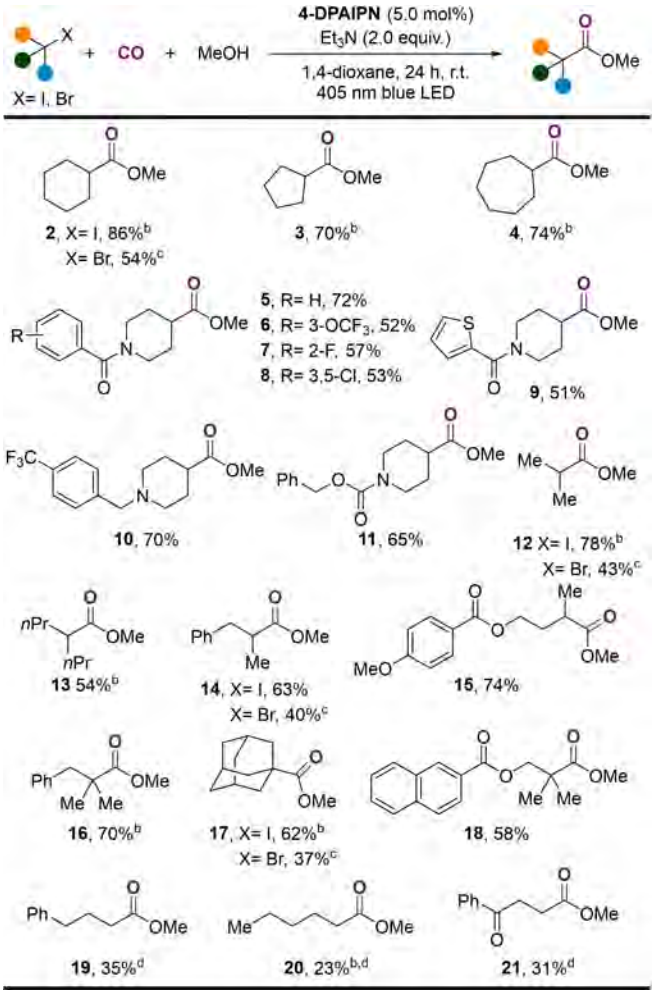

Figure 2. Substrate scope for alkyl iodides and bromides.[a] [a] Standard reaction conditions: alkyl halides (0.3 mmol), **4-DPAIPN** (5.0 mol%), Et_3N (0.6 mmol), CO (3.5 bar) and MeOH (0.2 mL) in 1,4-dioxane (1.0 mL) under a 405 nm blue LED at room temperature for 24 h. Isolated yields are given. [b] Yield was determined by GC using mesitylene as the internal standard. [c] DIPEA instead of Et_3N, 1,4-dioxane: MeCN (4:1) as solvent. [d] Bn_3N instead of Et_3N, THF as solvent.

able to isolate the carbonylation product (**2**, **12**, **15** and **17**) derived from secondary and tertiary bromides in moderate yield (37–54 %, respectively). Alkyl chlorides and fluorides were unreactive under these conditions (Figure S2).

Having demonstrated the potential of this approach for accessing various carboxylic acid derivatives from alkyl iodides and bromides, we proceeded to evaluate different nucleophiles in our system which can greatly improve the applicability of this strategy (Figure 3). We were pleased to see that different alcohols were compatible with this process. Primary alcohols gave the desired esters **22**–**26** in good yield (60–74 %, respectively). Moreover, we also succeeded in using secondary alcohols and phenols as nucleophiles under our conditions, as demonstrated by the formation of **27**–**29** (46–67 %, respectively).

Next, we considered the possibility of using amines as nucleophiles in this system, which is a known challenge in traditional carbonylations attributed to rapid β-hydride elimination in the alkyl-metal complex.[14] We found that primary amines such as benzylamine, furfurylamine, and aniline serve as nucleophiles, forming the desired amides **30**–**33** in useful yields (42–63 %, respectively). Notably, in all cases using primary amines as nucleophiles, imine formation was detected when the reactions were run under basic conditions (see Supporting Information for more details, Table S7). Therefore, an increase of equivalents of primary amines (from 3.0 to 4.0 equiv.) and change of the electron donor (from Et_3N to DIPEA) were necessary to achieve higher yield and conversion. Furthermore, our scope evaluation demonstrated broad compatibility with secondary amines including aliphatic and cyclic amines. We were successful in synthesizing the corresponding amides **34**–**37** in yield up to 68 %. Interestingly, when dibutylamine was both employed as the nucleophile and electron donor, primary iodides could undergo aminocarbonylation and the corresponding product **38** was obtained in 51 % yield. Additionally, only trace amounts of corresponding product were detected when thiol was used as the nucleophile (Figure S2).

To further demonstrate the synthetic versatility of this methodology, we evaluated several complex drug molecules and natural products as nucleophiles. The natural products (−)-menthol, cholesterol, and estrone gave the esters **39**–**41** in yields up to 67 %. Similarly, drug molecules mexiletine, leelamine, and desloratadine furnished the corresponding amides **42**–**44** in useful yield (42–55 %, respectively). More specifically, our strategy can be used in the synthesis of drug molecules, such as the antiparasitic medication praziquantel **45** in useful yield. Adamantyl amide **46** was synthesized in moderate yield, which has been reported to be a highly potent and selective 11β-HSD1 inhibitor.[15] Notably, the versatility of this metal-free strategy enables the synthesis of multiple drugs from simple building blocks, such as fenofibrate **48** and bezafibrate **49**.

^{13}C Incorporation. We next turned our attention to late-stage carbon isotope labeling. Stable isotopes (e.g., ^{13}C) are commonly used in conjunction with mass spectrometry for the quantification of the parent drug in biological samples.[16] Carbonylation with ^{13}CO has been developed as a valuable technique for late-stage incorporation of carbon isotopes as it typically displays excellent functional group tolerance.[17] We anticipated that the successful translation of the organocatalyzed carbonylation reaction strategy would therefore enable access to previously challenging or impossible to prepare radiotracers. To translate our method, we elected to use the commercially available Sila^{13}COgen as the ^{13}CO source in our system (Figure 4). Under the optimal conditions, ^{13}C-labeled esters (**50-^{13}C**) and amides (**51-^{13}C**) can be obtained in yields up to 72 %. Notably, it was possible to perform the reaction on a 2.0 mmol scale, where both compounds can be obtained in good yield (60 and 45 %, respectively).

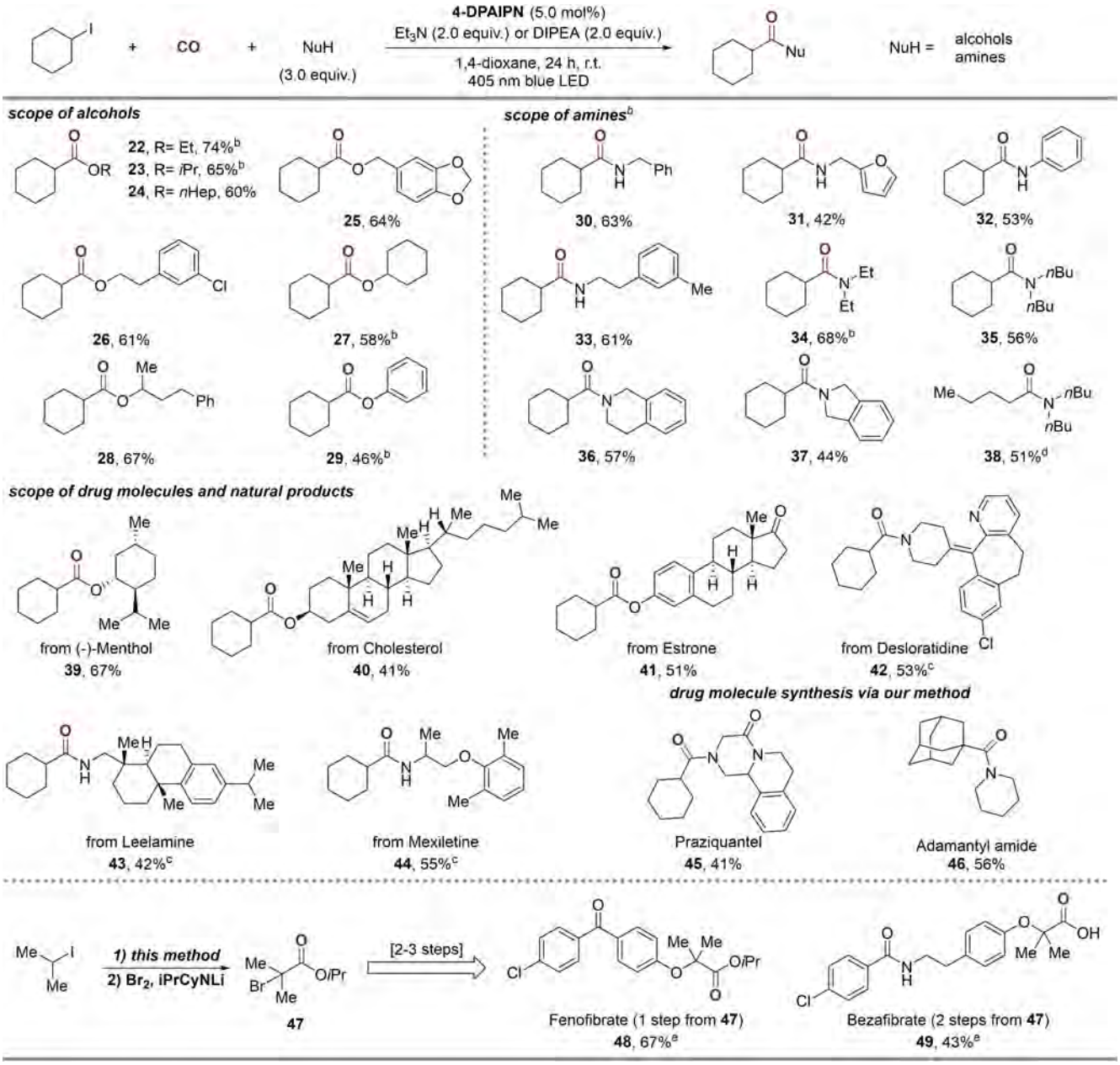

Figure 3. Substrate scope for different nucleophiles.[a] [a] Standard reaction conditions: **1** (0.3 mmol), **4-DPAIPN** (5.0 mol%), Et_3N (0.6 mmol), CO (3.5 bar) and nucleophile (0.9 mmol) in 1,4-dioxane (1.0 mL) under 405 nm blue LED at room temperature for 24 h. Isolated yields are given. [b] Yield was determined by GC using mesitylene as the internal standard. [c] Amines (1.2 mmol) and DIPEA (0.6 mmol) were used, and reaction time up to 36 h. [d] No DIPEA and yield determined by ^1H NMR using mesitylene as the internal standard. [e] See Supporting Information for detailed synthetic processes

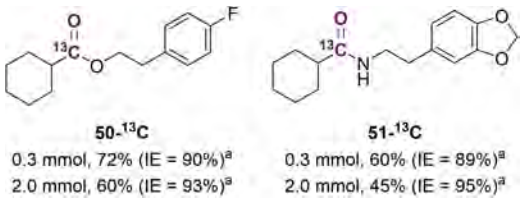

Figure 4. Synthesized products demonstrating application for carbon isotopic labeling. [a] Isotopic enrichments (IE) were determined by mass spectrometry.

Mechanistic Investigation. The mechanistic details of this reaction are intriguing because the organic photocatalyst **4-DPAIPN** can promote different reaction pathways.[18] To elucidate potential mechanisms, we performed density functional theory (DFT) calculations to investigate the kinetics and thermodynamics of possible pathways and to estimate barriers for single electron-transfer (SET). We used M06-2X/def2-TZVP//B3LYP-D3(BJ)/def2-SVP calculations with an SMD description of

dioxane solvation: a complete description of computational methods is detailed in Supporting Information.

The standard reduction potentials (vs SCE) have previously been theoretically estimated for primary, secondary and tertiary alkyl halides in acetonitrile: $E^{o}_{RX/R^{\bullet}+X^{-}}$ lies in the range of −0.85 to −0.92 V for iodides, −1.0 to −1.08 V for bromides, and −1.17 to −1.19 V for chlorides.[19] Exergonic reduction of alkyl bromide and iodide substrates is possible from **4-DPAIPN**$^{\bullet-}$ (oxidation potential of +1.10 V).[20] Reduction of **1** results in irreversible heterolytic C–I cleavage, forming the cyclohexyl radical. We considered competitive pathways for product formation with Et_2NH as a model nucleophile (Figure 5a). Different pathways were categorized either as non-chain processes or chain processes. Pathways classified as non-chain processes do not involve a radical propagation step and afford an acylium ion intermediate that can be intercepted by the nucleophile. For chain processes, we considered both a radical propagation step involving another molecule of alkyl iodide or an SET step involving $Et_3N^{\bullet+}$. Computed thermodynamic and kinetic parameters are shown in Figure 5a, and the geometries of key transition structures (TSs) are shown in Figure 5b.

We investigated two distinct non-chain processes, (Figure 5a, pathways A and B). In path A, at this level of theory

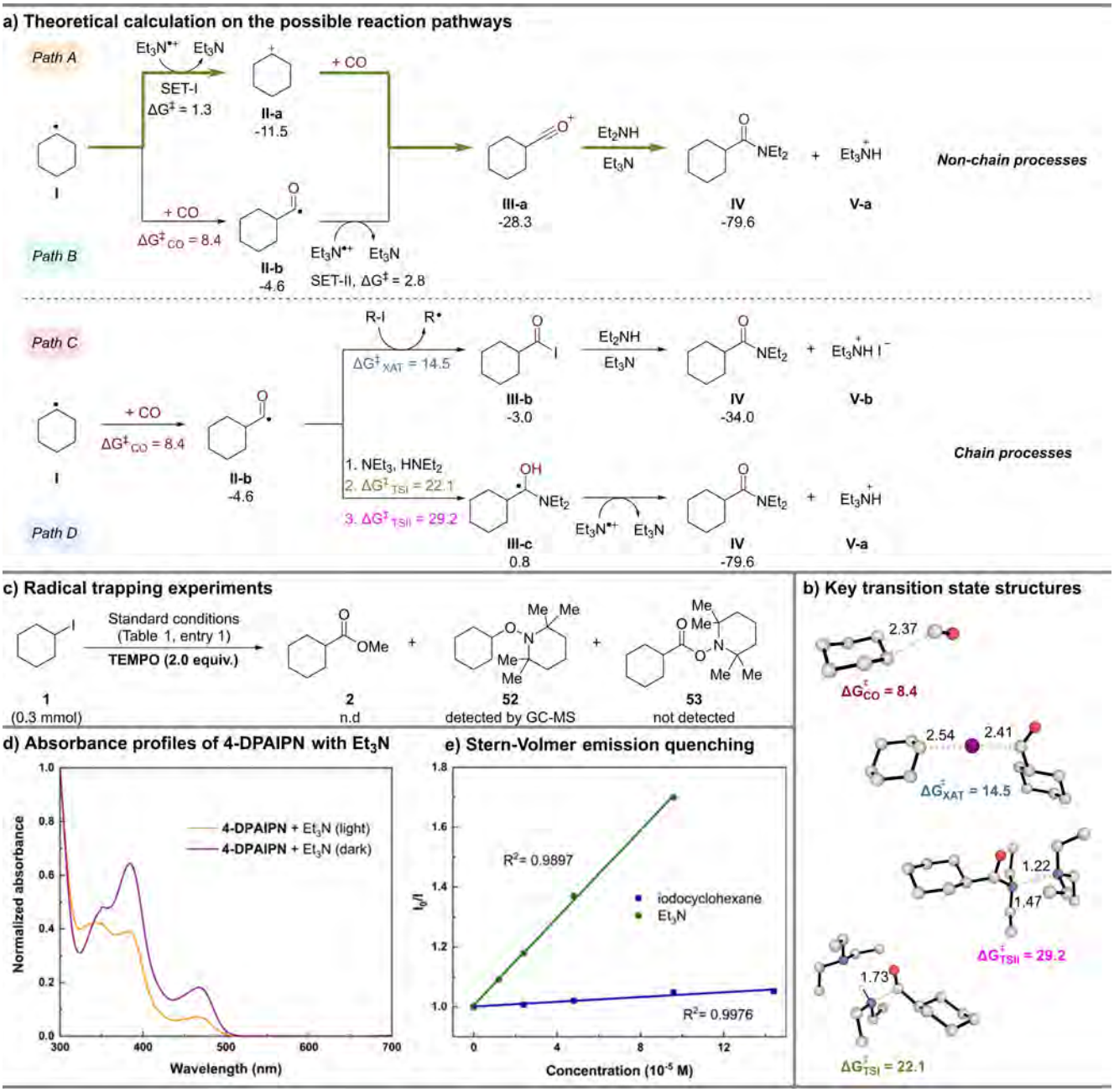

Figure 5. Overview of mechanistic studies.

we found the oxidation of alkyl radical **I** via single electron transfer (SET) with $Et_3N^{\bullet+}$, forming carbocationic intermediate **II-a**, to be exergonic ($\triangle G = -11.5$ kcal/mol). The SET barrier ($\triangle G^{\ddagger} = 1.3$ kcal/mol), estimated from classical Marcus theory (via Nelsen's 4-point method) is also small. Subsequently, carbocation **II-a** reacts with CO, forming acylium ion intermediate **III-a** and this step is predicted to occur favorably ($\triangle G_{rel} = -28.3$ kcal/mol). Scans along the potential energy surface (Figure S3) suggest that this step is energetically barrierless. Reaction of the amine nucleophile with the acylium electrophilic forms product **IV**, which is highly exergonic ($\triangle G_{rel} = -79.6$ kcal/mol). Based on the computed free energies and estimated barriers of single-electron transfer, this pathway is both kinetically and thermodynamically highly feasible. Path B differs by the order of CO addition and SET steps. First, an acyl radical is generated via nucleophilic radical addition of the alkyl radical to CO. This step is exergonic ($\triangle G_{rel} = -4.6$ kcal/mol) with a barrier for this radical addition TS of 8.4 kcal/mol. The newly formed acyl radical **II-b** can then undergo oxidation via SET with $Et_3N^{\bullet+}$ to produce an acylium ion intermediate **III-a**. This single-electron oxidation is exergonic ($\triangle G_{rel} = -28.3$ kcal/mol) with a 2.8 kcal/mol estimated Marcus barrier. At this point, path B converges to the same acylium ion intermediate as path A. While both pathways are feasible, based on carbocation stabilities we expect that path A is favored for tertiary and secondary substrates as in Figure 5a, but will be inaccessible for primary substrates, which will favor path B.

We also considered the possibility of radical propagation via a chain process for the same substrate (Figure 5a, pathway C) or single electron transfer (Figure 5a, pathway D). These pathways involve the proposed acyl radical intermediate **II-b**. In path C, the corresponding carbonyl product is formed via ATC,[21] in which **II-b** can react with another alkyl iodide substrate via halogen atom transfer (XAT) to generate acyl iodide **III-b**. In general, XAT is presumed to be the rate determining step in ATC processes. Computationally, we located the XAT TS, which has a barrier of 14.5 kcal/mol relative to **II-b**. The XAT step is computed to be exergonic ($\triangle G_{rel} = -3.0$ kcal/mol) and regenerates an alkyl radical that can reenter this pathway. The electrophilic intermediate **III-b** can undergo nucleophilic addition by an amine or alcohol nucleophile to afford the corresponding carbonyl product in exergonic fashion ($\triangle G_{rel} = -34.0$ kcal/mol). In path D, we considered that the addition of amine or alcohol to the acyl radical could occur via amine-assisted intramolecular proton transfer to afford **III-c** (Path D).[7] Acyl radicals are themselves nucleophilic and so, accordingly, this pathway incurs a high overall activation barrier. Further, we found that the involvement of a second amine molecule to act as base was necessary to obtain energy minima along this pathway. Geometries of these complexes are shown in Figure S5. Endergonic C–N bond formation ($\triangle G_{rel} = 16.3$ kcal/mol) occurs with a barrier of 22.1 kcal/mol, and is followed by amine-assisted proton transfer to generate the carbinolamine radical adduct. This TS has a barrier of 29.2 kcal/mol, and the formation of the α-hydroxy radical intermediate is moderately endergonic ($\triangle G_{rel} = 0.8$ kcal/mol). However, net product formation from the oxidation of the α-hydroxy radical intermediate via single electron transfer with $Et_3N^{\bullet+}$ is largely exergonic ($\triangle G_{rel} = -79.6$ kcal/mol). Overall, the high barriers for path D suggest that it is not kinetically feasible, whereas Paths B and C are both thermodynamically and kinetically feasible.

Several experiments were performed that further support these mechanistic hypotheses. First, under standard conditions, **52** was detected by GC-MS when TEMPO was used as a radical trap (Figure 5c). However, acyl radical **53** was not observed, which suggests that paths B, C, and D are not prevalent. Second, we probed the generation of **4-DPAIPN** radical anion via UV/Vis experiments. We irradiated a mixture of **4-DPAIPN** and Et_3N while monitoring speciation by absorption spectroscopy (Figure 5d). This reaction resulted in a decrease in **4-DPAIPN** features and growth of new features consistent with radical anion formation. This observation is in agreement with study by Wickens and co-workers who observed **4-DPAIPN**$^{\bullet-}$ from irradiation of **4-DPAIPN** and sodium formate.[22] Indeed, ^{1}H NMR experiments also support the formation of **4-DPAIPN**$^{\bullet-}$ (Figure S8). Third, Stern–Volmer quenching studies demonstrated one-electron transfer between **4-DPAIPN*** and Et_3N but not the iodide for the initiation process. These results are agreement with previous studies which both support a visible-light-induced two-electron reduction process by way of sequential electron transfer.[23]

Based on our mechanistic investigations, computational studies, and previous literature reports we propose a possible reaction mechanism (Figure 6).[7,19–24] Under blue light irradiation, **4-DPAIPN** produces the excited state species **4-DPAIPN*** which undergoes a SET process with Et_3N to provide the intermediate **4-DPAIPN**$^{\bullet-}$ and $Et_3N^{\bullet+}$. Then, **4-DPAIPN**$^{\bullet-}$ reduces the alkyl iodide to the alkyl radical a which can undergo single-electron oxidation with

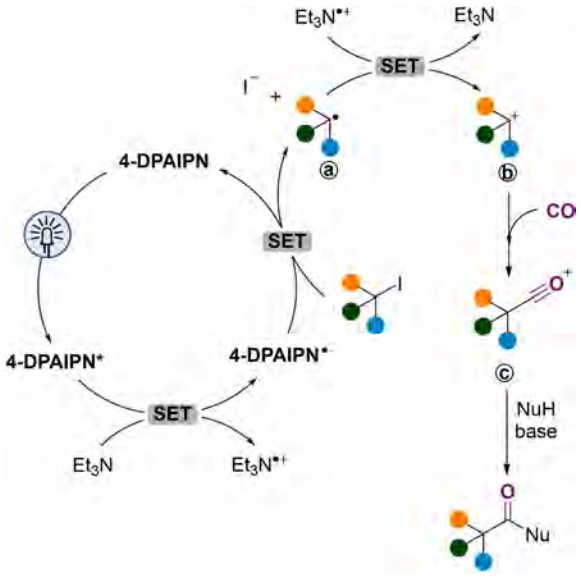

Figure 6. Proposed mechanism.

$Et_3N^{\bullet+}$ to form a carbocation intermediate b. Intermediate b can readily trap carbon monoxide to generate an acylium ion intermediate c. Lastly, product formation occurs from the nucleophilic addition of alcohols or amines to the reactive acylium ion intermediate c in the presence of base (Et_3N).

Conclusion

Overall, we have developed an organocatalyzed carbonylation methodology which can transform alkyl halides to esters and amides under metal-free conditions. The utilization of this strategy eliminates the requirement for transition metal catalysts in carbonylation reactions under visible light. Importantly, this protocol can serve as a method for synthesis of carbon isotope labeled carbonyl compounds. Preliminary mechanistic studies, including radical trapping, quenching experiments, and DFT calculations, provide insights into the catalytic cycle.

Acknowledgements

This work was supported by the National Science Foundation Center for Chemical Innovation (NSF-CCI) Center for Sustainable Photoredox Catalysis (SuPRCat) under Award 2318141. We are grateful for the resources available through the Analytical Resources Core (RRID: SCR_021758) and thank Dr. Duo Wei for his advice on testing the CO gas pressure. Computational resources were supported by the Alpine high performance computing resource, jointly funded by the University of Colorado Boulder, the University of Colorado Anschutz, and Colorado State University, and the Advanced Cyberinfrastructure Coordination Ecosystem: Services & Support (ACCESS) through allocations TG-CHE180056 and TG-CHE240044.

Conflict of Interest

The authors declare no conflict of interest.

Data Availability Statement

The data that support the findings of this study are available in the supplementary material of this article.

Keywords: carbonylation · alkyl halides · visible light · organic photoredox catalysis · carbon isotope

[1] a) J.-B. Peng, H.-Q. Geng, X.-F. Wu, *Chem.* **2019**, *5*, 526–552; b) R. Franke, D. Selent, A. Börner, *Chem. Rev.* **2012**, *112*, 5675–5732; c) A. Brennführer, H. Neumann, M. Beller, *Angew. Chem. Int. Ed.* **2009**, *48*, 4114–4133; d) M. Beller, B. Cornils, C. D. Frohning, C. W. Kohlpaintner, *J. Mol. Catal. A* **1995**, *104*, 17–85.

[2] J. Singh, S. Sharma, A. Sharma, *J. Org. Chem.* **2021**, *86*, 24–48.

[3] a) T. Kondo, Y. Tsuji, Y. Watanabe, *Tetrahedron Lett.* **1988**, *29*, 3833–3836; b) J.-J. Brunet, C. Sidot P Caubere, *Tetrahedron Lett.* **1981**, *22*, 1013–1016; c) V. Dragojlovic, D. B. Gao, Y. Chow, *J. Mol. Catal. A* **2001**, *171*, 43–51; d) D. Cash, A. Combs, V. Dragojlovic, *Tetrahedron Lett.* **2004**, *45*, 1143–1145; e) L. Z. Mu, Y. P. Jia, J. M. Yin, G. Y. Zhou, Y. N. Cui, D. B. Gao, *Chin. Chem. Lett.* **2009**, *20*, 531–534; f) I. Ryu, S. Kreimerman, F. Araki, S. Nishitani, Y. Oderaotoshi, S. Minakata, M. Komatsu, *J. Am. Chem. Soc.* **2002**, *124*, 3812–3813; g) T. Fukuyama, S. Nishitani, T. Inouye, K. Morimoto, I. Ryu, *Org. Lett.* **2006**, *8*, 1383–1386; h) A. Fusano, S. Sumino, T. Fukuyama, I. Ryu, *Org. Lett.* **2011**, *13*, 2114–2117.

[4] K. Nagahara, I. Ryu, M. Komatsu, N. Sonoda, *J. Am. Chem. Soc.* **1997**, *119*, 5465–5466.

[5] a) W. H. Zhong, Y. N. Cui, S. M. Li, Y. P. Jia, J. M. Yin, *Chin. Chem. Lett.* **2012**, *23*, 29–32; b) A. M. Veatch, E. J. Alexanian, *Chem. Sci.* **2020**, *11*, 7210–7213.

[6] a) S. J. Ton, K. T. Neumann, P. Nørby, Y. Skrydstrup, *J. Am. Chem. Soc.* **2021**, *143*, 17816–17824; b) S. S. Pedersen, A. S. Donslund, J. H. Mikkelsen, O. S. Bakholm, F. Papp, K. B. Jensen, M. B. F. Gustafsson, T. Skrydstrup, *Chem. Eur. J.* **2021**, *27*, 7117–7123.

[7] a) J. A. Forni, N. Micic, T. U. Connell, G. Weragoda, A. Polyzos, *Angew. Chem. Int. Ed.* **2020**, *59*, 18646–18654; b) S. Y. Chow, M. Y. Stevens, L. Akerbladh, S. Bergman, L. R. Odell, *Chem. Eur. J.* **2016**, *22*, 9155–9161.

[8] Y.-H. Zhao, X.-W. Gu, X.-F. Wu, *Org. Chem. Front.* **2024**, *11*, 442–447.

[9] M. Sardana, J. Bergman, C. Ericsson, L. P. Kingston, M. Schou, C. Dugave, D. Audisio, C. S. Elmore, *J. Org. Chem.* **2019**, *84*, 16076–16085.

[10] G. M. Torres, Y. Liu, B. A. Arndtsen, *Science* **2020**, *368*, 318–323.

[11] K. E. Chami, Y. Liu, M. A. Belahouane, Y. Ma, P. Lagueux-Tremblay, B. A. Arndtsen, *Angew. Chem. Int. Ed.* **2020**, e202213297.

[12] a) J. C. Theriot, C.-H. Lim, H. Yang, M. D. Ryan, C. B. Musgrave, G. M. Miyake, *Science* **2016**, *352*, 1082–1086; b) D. F. Chen, B. M. Boyle, B. G. McCarthy, C.-H. Lim, G. M. Miyake, *J. Am. Chem. Soc.* **2019**, *141*, 13268–13277; c) J. P. Cole, D. F. Chen, M. Kudisch, R. M. Pearson, C.-H. Lim, G. M. Miyake, *J. Am. Chem. Soc.* **2020**, *142*, 13573–13581; d) C. H. Chrisman, M. Kudisch, K. O. Puffer, T. K. Stewart, Y. M. L. Lamb, C.-H. Lim, R. Escobar, P. Thordarson, J. W. Johannes, G. M. Miyake, *J. Am. Chem. Soc.* **2023**, *145*, 12293–12304.

[13] a) F. Juliá, T. Constantin, D. Leonori, *Chem. Rev.* **2022**, *122*, 2292–2352; b) N. Noto, S. Saito, *ACS Catal.* **2022**, *12*, 15400–15415; c) N. A. Romero, D. A. Nicewicz, *Chem. Rev.* **2016**, *116*, 10075–10166; d) Y. Lee, M. S. Kwon, *Eur. J. Org. Chem.* **2020**, *38*, 6028–6043; e) J. Xu, J. Cao, X. Wu, H. Wang, X. Yang, X. Tang, R. Toh, R. Zhou, E. K. L. Yeow, J. Wu, *J. Am. Chem. Soc.* **2021**, *143*, 13266–13273.

[14] a) L. Wu, X. Fang, Q. Liu, R. Jackstell, M. Beller, X.-F. Wu, *ACS Catal.* **2014**, *4*, 2977–2989; b) X. Wu, Y. Zhao, H. Ge, *J. Am. Chem. Soc.* **2015**, *137*, 4924–4927.

[15] S. P. Webster, P. Ward, M. Binnie, E. Graigie, K. M. M. McConnell, K. Sooy, A. Vinter, J. R. Seckl, B. R. Walker, *Bioorg. Med. Chem. Lett.* **2007**, *17*, 2838–2843.

[16] T. W. Fan, P. Lorkiewicz, K. Sellers, H. N. B. Moseley, R. M. Higashi, A. N. Lane, *Pharmacol. Ther.* **2012**, *133*, 366–391.

[17] a) S. D. Friis, A. T. Lindhardt, T. Skrydstrup, *Acc. Chem. Res.* **2016**, *49*, 594–605; b) D. U. Nielsen, K. T. Neumann, A. T. Lindhardt, T. Skrydstrup, *J. Labelled Compd. Radiopharm.* **2018**, *61*, 949–987.

[18] a) P. P. Singh, V. Srivastava, *Org. Biomol. Chem.* **2021**, *19*, 313–321; b) S. N. Alektiar, Z. K. Wickens, *J. Am. Chem. Soc.* **2021**, *143*, 13022–13028; c) L. Chen, Q. Qu, C.-K. Ran, W. Wang, W. Zhang, Y. He, L.-L. L, J.-H. Ye, D.-G. Yu, *Angew. Chem. Int. Ed.* **2023**, *62*, e202217918.
[19] A. A. I, C. Y. Lin, M. L. Coote, A. Gennaro, *J. Phys. Chem. B* **2011**, *115*, 678–684.
[20] J. Luo, J. Zhang, *ACS Catal.* **2016**, *6*, 873–877.
[21] a) S. S, A. F, T. F, I. Ryu, *Acc. Chem. Res.* **2014**, *47*, 1563–1574; b) H. Masubara, I. Ryu, C.-H. Schiesser, *Org. Biomol. Chem.* **2007**, *5*, 3320–3324.
[22] A. F. Chmiel, O. P. Williams, C. P. Chernowsky, C. S. Yeung, Z. K. Wickens, *J. Am. Chem. Soc.* **2021**, *143*, 10882–10889.
[23] T. Ju, Y.-Q. Zhou, K.-G. Cao, Q. Fu, J.-H. Ye, G.-Q. Sun, X.-F. Liu, L. Chen, L.-L. Liao, D.-G. Yu, *Nat. Catal.* **2021**, *4*, 304–311.
[24] F. Zhao, H.-J. Ai, X.-F. Wu, *Chin. J. Chem.* **2021**, *39*, 927–932.

Manuscript received: June 10, 2024
Accepted manuscript online: August 7, 2024
Version of record online: October 30, 2024